

Supporting Information

Acceleration of Oral Wound Healing under Diabetes Mellitus by Bio-adhesive Hydrogel

Jiwei Sun, PhD^{1,2,3†}, Tiantian Chen, PhD^{5†}, Baoying Zhao, MS^{1,2,3†}, Wenjie Fan, MS^{1,2,3}, Yufeng Shen, PhD^{1,2,3}, Haojie Wei, MS⁴, Man Zhang, MS^{1,2,3}, Wenhao Zheng, PhD^{1,2,3}, Jinfeng Peng, PhD^{1,2,3}, Jinyu Wang, PhD^{1,2,3}, Yifan Wang, PhD^{1,2,3}, Lihong Fan, PhD⁴, Yingying Chu, PhD^{4*}, Lili Chen, PhD^{1,2,3*}, Cheng Yang, PhD^{1,2,3*}

¹Department of Stomatology, Union Hospital, Tongji Medical College, Huazhong University of Science and Technology, Wuhan 430022, China

²School of Stomatology, Tongji Medical College, Huazhong University of Science and Technology, Wuhan 430030, China

³Hubei Province Key Laboratory of Oral and Maxillofacial Development and Regeneration, Wuhan 430022, China

⁴School of Chemistry, Chemical Engineering and Life Sciences, Wuhan University of Technology, Wuhan 430070, P. R. China.

⁵School of Resources and Environmental Engineering, Wuhan University of Technology, Wuhan 430070, China

***Emails:** y.chu@whut.edu.cn (Yingying Chu)

chenlili1030@hust.edu.cn (Lili Chen)

yangc715@126.com (Cheng Yang)

Supplementary Figures and Figure Legends

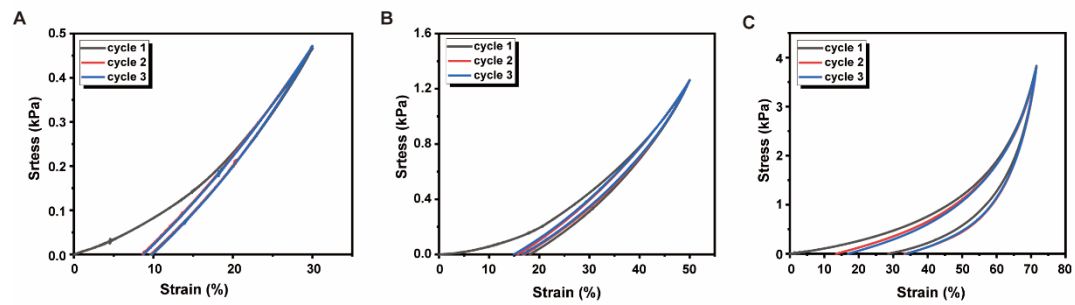


Figure S1. Repeated compressive tests of the Fe-TA@ P(AM-AA) hydrogel three times at A)30%, B)50%, and C)70% strain, separately.

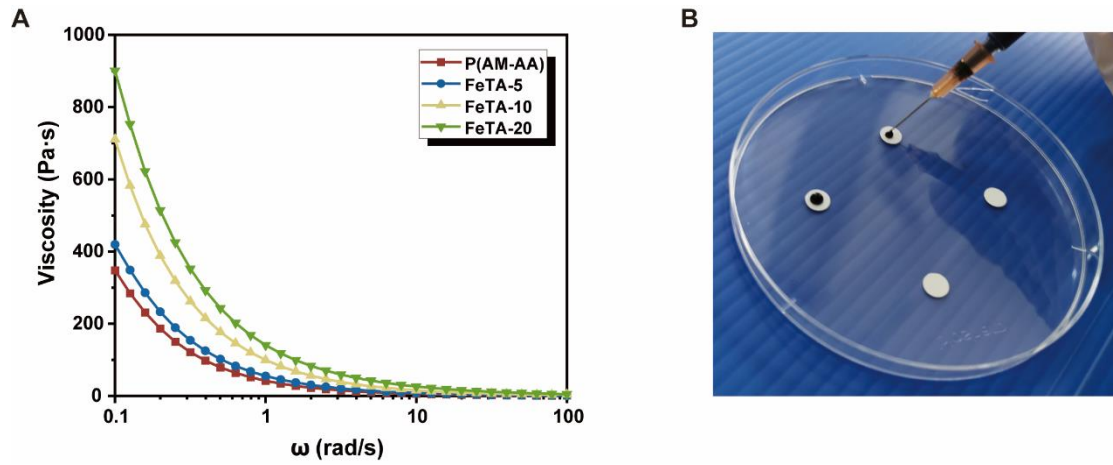


Figure S2. Injectability properties of the Fe-TA@ P(AM-AA) hydrogel.

A) Shear-thinning behavior of the Fe-TA@ P(AM-AA) hydrogel.

B) Photograph of injectability properties of the Fe-TA@ P(AM-AA) hydrogel.

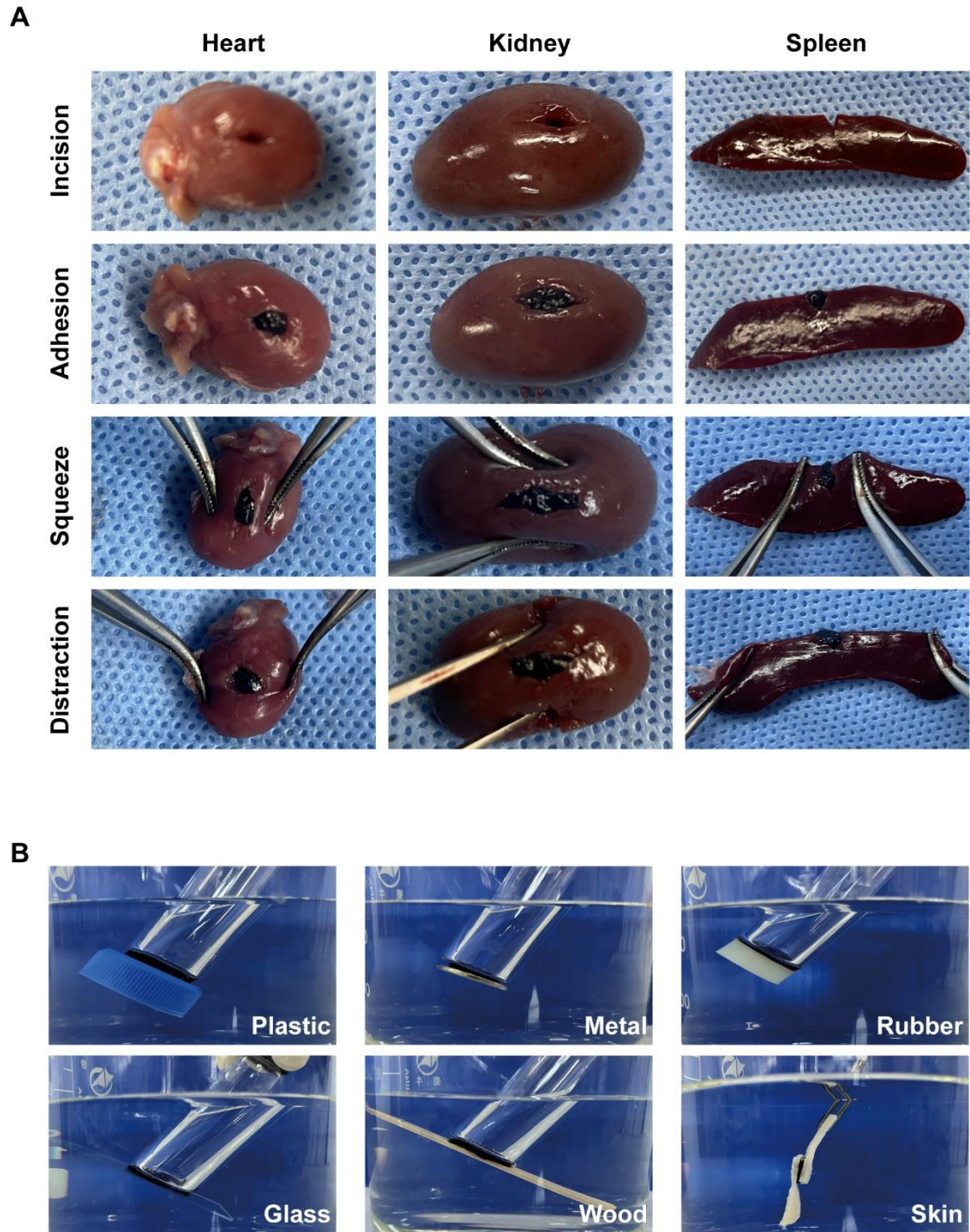


Figure S3. Wet adhesion of Fe-TA@P(AM-AA).

A) Photographs of the adhesiveness of Fe-TA@P(AM-AA) (10%wt) hydrogel to the incisions on fresh rat heart, kidney and spleen.

B) Photographs of the adhesiveness of Fe-TA@P(AM-AA) (10%wt) hydrogel to different materials.

Relaxed



Figure S4. Fe-TA@P(AM-AA) remained adhering on the surface of wet rat tongue after tongue movement.

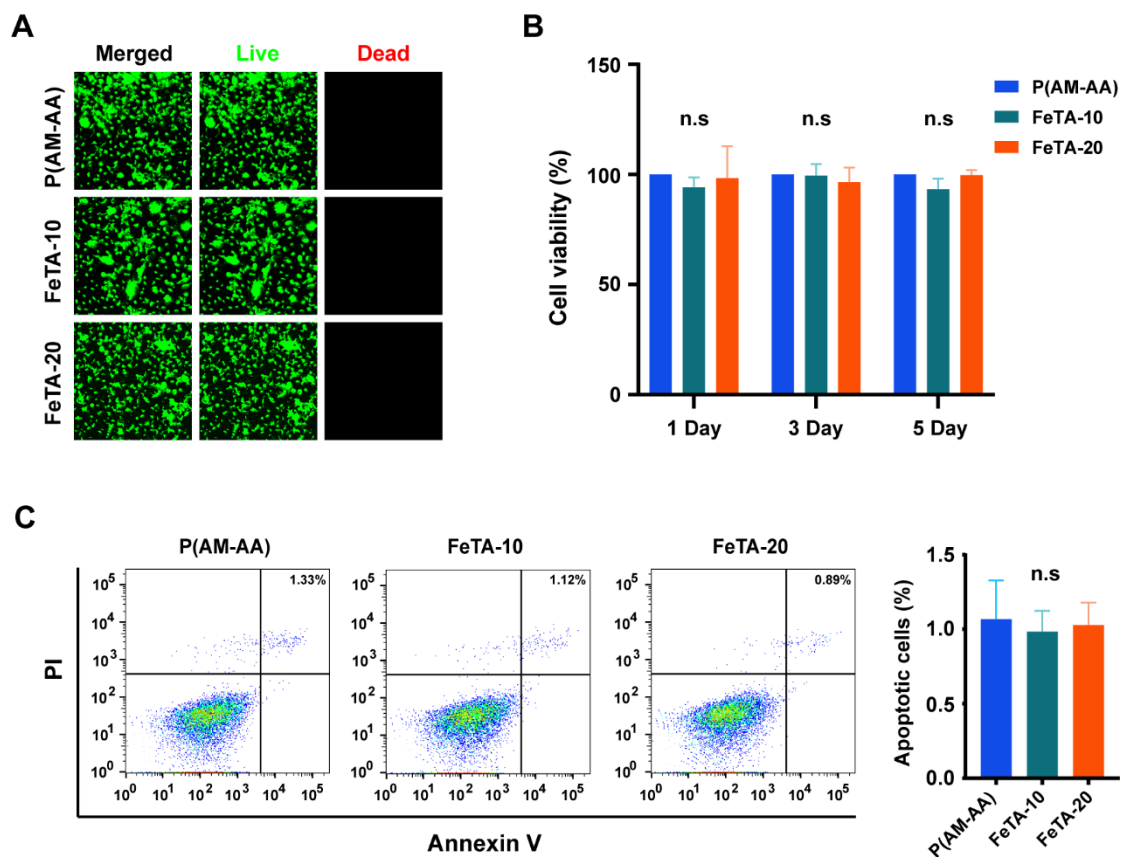


Figure S5. Cytocompatibility of the Fe-TA@P(AM-AA) hydrogel.

A) Live/Dead staining fluorescent images of oral epithelial cells after incubation with the Fe-TA@P(AM-AA) extracts under high glucose medium for 48 h.

B) Oral epithelial cells were co-cultured with Fe-TA@P(AM-AA) extracts under high glucose medium, and cell proliferation activity was assessed with CCK-8 assays after 1, 3 and 5 days.

C) Apoptosis status of oral epithelial cells measured by Annexin V/PI flow cytometry analysis.

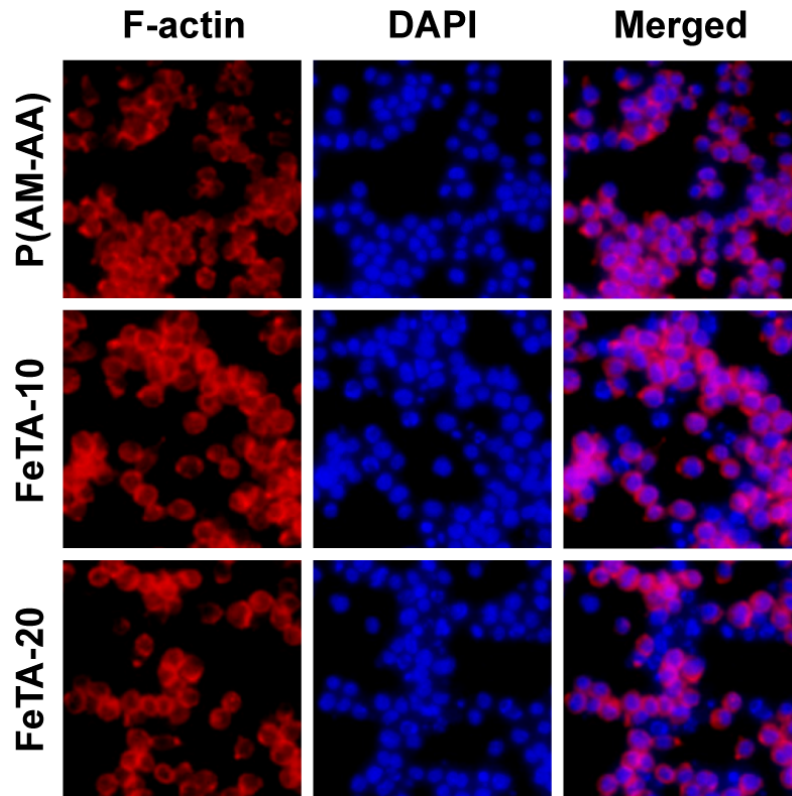
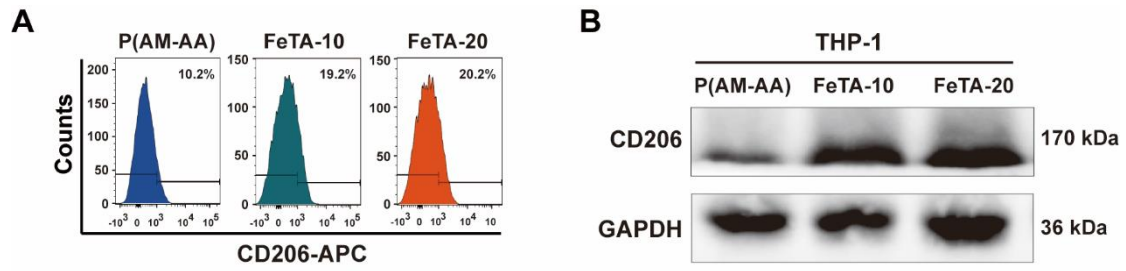


Figure S6. Cell adhesion and spreading on composite hydrogels.

Cytoskeletal staining of macrophages co-cultured with Fe-TA@P(AM-AA) extracts for 48 h.



5

Figure S7. Immunomodulatory potential of composite hydrogels on macrophage polarization

A) Flow cytometry analysis of the percentage of CD206+ M2 macrophages.

B) Western blotting analysis of the protein expression level of M2 marker CD206.

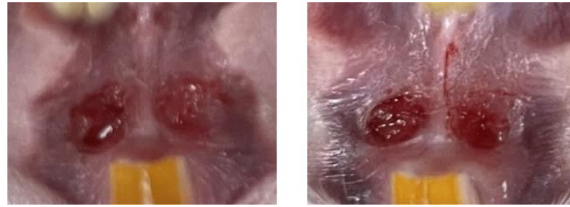


Figure S8. Oral mucosa defects above the muscle tissue with the same size (1.2 mm diameter) were created in the diabetic rat.

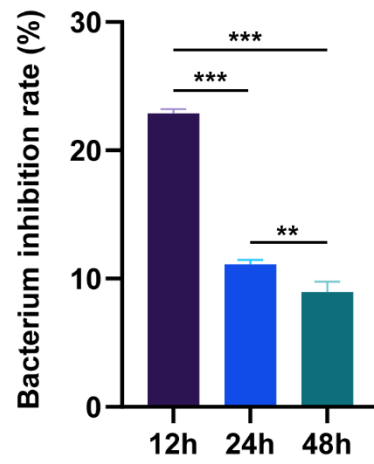


Figure S9. Antibacterial effect of Fe-TA@P(AM-AA) gel on rat oral mucosa defects were analyzed at different time points.

Supplementary Tables

Table 1 Primers and parameters used for the PCR analysis

Gene Name	Primer sequence
<i>h-IL10</i>	Forward: 5'-GACTTTAAGGGTTACCTGGGTTG -3' Reverse: 5'-TCACATGCGCCTTGATGTCTG -3'
<i>h-IL4</i>	Forward: 5'-AGGCTGAAAGGGGGAAAGC -3' Reverse: 5'-CTGTTCACCTCAACTGCTCC -3'
<i>h-CCL2</i>	Forward: 5'-ATCCAGCACACGAATACACA -3' Reverse: 5'-AAAGTTCTTTGAGTTGCGGC -3'
<i>h-IL1β</i>	Forward: 5'-ATGATGGCTTATTACAGTGGCAA -3' Reverse: 5'-GTCGGAGATTCGTAGCTGGA -3'
<i>h-IL6</i>	Forward: 5'-ACTCACCTCTTCAGAACGAATTG -3' Reverse: 5'-CCATCTTTGGAAGGTTTCAGGTTG -3'
<i>h-TNFα</i>	Forward: 5'-CCTCTCTCTAATCAGCCCTCTG -3' Reverse: 5'-GAGGACCTGGGAGTAGATGAG -3'